

SHAPE : Self-Improved Visual Preference Alignment by Iteratively Generating Holistic Winner

Kejia Chen^{*1} Jiawen Zhang^{*1} Jiacong Hu¹ Jiazhen Yang¹ Jian Lou² Zunlei Feng¹ Mingli Song¹

¹Zhejiang Univerisity ²Sun Yat-sen University

Abstract

Large Visual Language Models (LVLMs) increasingly rely on preference alignment to ensure reliability, which steers the model behavior via preference fine-tuning on preference data structured as “image - winner text - loser text” triplets. However, existing approaches often suffer from limited diversity and high costs associated with human-annotated preference data, hindering LVLMs from fully achieving their intended alignment capabilities. We present SHAPE, a self-supervised framework capable of transforming the already abundant supervised text-image pairs into holistic preference triplets for more effective and cheaper LVLM alignment, eliminating the need for human preference annotations. Our approach facilitates LVLMs in progressively enhancing alignment capabilities through iterative self-improvement. The key design rationale is to devise preference triplets where the winner text consistently improves in holisticness and outperforms the loser response in quality, thereby pushing the model to “strive to the utmost” of alignment performance through preference fine-tuning. For each given text-image pair, SHAPE introduces multiple visual augmentations and pairs them with a summarized text to serve as the winner response, while designating the original text as the loser response. Experiments across 12 benchmarks on various model architectures and sizes, including LLaVA and DeepSeek-VL, show that SHAPE achieves significant gains, for example, achieving +11.3% on MMVet (comprehensive evaluation), +1.4% on MMBench (general VQA), and +8.0% on POPE (hallucination robustness) over baselines in 7B models. Notably, qualitative analyses confirm enhanced attention to visual details and better alignment with human preferences for holistic descriptions.

1. Introduction

Inheriting the breakthroughs in large language models (LLMs), large visual language models (LVLMs) have devel-

oped rapidly and achieved astounding performance on a wide range of image-text understanding tasks, showcasing exceptional potential [1, 27, 28, 57]. Despite their remarkable capabilities, there persists significant challenges in aligning LVLMs’ generations with human preferences, where models produce texts that diverge from visual inputs and human expectations [6, 39]. Failure to achieve such preference alignments could lead to serious consequences for LVLMs’ real-world applications, ranging from the spread of misinformation to the risk of harmful decision-making.

Given the critical role of preference alignment, there has been a surge in research interest in addressing the hurdles of aligning LVLMs’ generations with human preferences. The seminal approach involves first collecting large-scale preference data and human annotations, then utilizing preference fine-tuning algorithms such as reinforcement learning with human feedback (RLHF) or more recent direct preference optimization (DPO) based on preference triplets [4, 5, 25, 39]. This approach can be resource-intensive, as human annotation can be demanding and costly. Additionally, it may struggle to achieve comprehensive coverage of all possible distributions of human preferences. To remedy these limitations in the requirement of human-annotated preference data, alternative approaches propose leveraging external LVLMs like GPT-4 to generate preference data. However, this approach introduces new challenges: inconsistent scoring mechanisms and discrete metrics hinder accurate capability assessment [3, 19, 51]. Additionally, relying on external models for scoring is both costly and limited in capturing the nuanced semantic relationships between visual and textual content. As a result, the preference alignment efforts of existing LVLMs are hindered by the challenge of acquiring high-quality and cost-efficient preference data.

Recognizing the scarcity of preference data as a critical bottleneck [43, 45] limiting LVLMs alignment performance, recent studies have sought to mitigate this challenge, primarily by generating LVLMs-aligned preference data using LLMs to reduce reliance on labeled data. For instance, SIMA [42] extracts images and question from visual input and lets the model generate responses, and then uses a self-

^{*}Equal contribution.

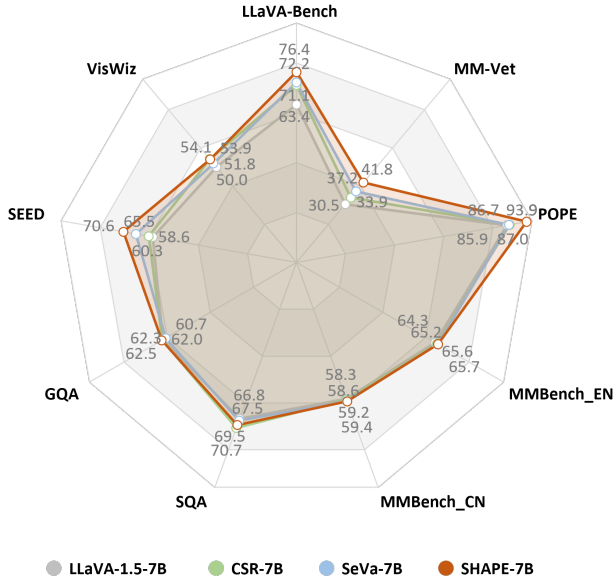


Figure 1. Comprehensive evaluation of SHAPE’s enhanced performance against SOTA models across multimodal benchmarks: Achieving +11.3% on MMVet, +1.4% on MMBench, and +8.0% on POPE over baselines in 7B Models.

assessment scheme to create preference pairs for training. While CSR [56] implements a reward mechanism for model self-generation and calibration. SEVA [60] incorporates DPO for preference alignment but relies solely on comparing raw and enhanced versions of the model’s visual outputs, limiting its ability to capture rich semantic connections.

By and large, these recent attempts devise the preference data by exclusively focusing on introducing multiple text-side operations, while leaving the image-side fixed during the winner and loser samples generation [20], which overlooks the crucial visual-textual semantic interplay. Our experiments demonstrate that LVLMs are highly sensitive to image-side modifications, such as random flips, which can lead to substantial semantic shifts in model outputs [16, 58–60]. This **observation** transforms a perceived limitation into an opportunity. This sensitivity, rather than being a drawback, offers a supervisory signal to generate diverse, semantically related text responses without additional human preference annotations, thereby yielding high-quality and cost-efficient preference triplets for LVLMs’ alignment. By leveraging visual augmentation-induced variations to create preference pairs automatically, we can construct rich semantic comparisons while preserving the crucial visual-textual semantic interplay. Therefore, we address a fundamental question in LVLMs preference alignment: *How can we leverage existing supervised annotation data to automatically construct high-quality preference pairs while maintaining low annotation costs and ensuring holistic semantic understanding?*

To tackle these challenges, we propose **SHAPE** (Self-improved **H**olistic **A**lignment for **P**reference **E**nhancement), a novel framework that optimizes LVLMs preference alignment through automated construction of competitive preference pairs. Our design rationale stems from a key observation: effective preference alignment requires carefully crafted pairs that serve two critical properties: **1. A winner text that exemplifies superior quality; 2. A competitive loser that is already capable of providing meaningful enough learning signals.** This deliberate construction ensures effective preference alignment while eliminating the need for costly manual annotations.

Main Contributions and Results. Recognizing the inherent limitations in the knowledge depth and reasoning capabilities of single LVLMs, as well as the negative responses triggered by image-side augmentation strategies, which highlight the need for a more robust approach to preference alignment, we propose **SHAPE**, a novel self-improved framework that leverages the intrinsic relationships between visual and textual modalities. By synthesizing stronger responses through summarization and augmentation-aware mechanisms, **SHAPE** ensures both robustness and semantic coherence. Furthermore, our framework constructs holistic preference pairs by generating “winners” from diverse candidate outputs, dynamically improving alignment with preferred behaviors while minimizing annotation costs. Extensive evaluations conducted across 12 benchmarks demonstrate the effectiveness of our approach, achieving substantial performance gains of 10.36%, 6.46%, 2.3% and 3.3% on the MMVet benchmark for LLaVA-1.5-7B, 13B and DeepSeek-VL2-3B, 27B model variants respectively, thereby surpassing state-of-the-art results while effectively addressing the limitations of single-model reasoning and the challenges associated with augmentation strategies.

2. Related Work

2.1. Large Visual Language Models

Recent years have witnessed remarkable progress in Visual Language Models (LVLMs), from early pioneers like CLIP to advanced models like BLIP, LLaVA, and InstructBLIP [11, 23, 28, 47]. These models leverage image-text pretraining to achieve sophisticated multimodal understanding, with recent advances incorporating efficient pseudo-labels for complex visual reasoning tasks, such as Kosmos-2 and PaLI-X [8, 32].

Despite these advances, LVLMs still face significant challenges in real-world applications, particularly in domain-specific tasks and cross-scenario generalization. Researchers have explored various enhancement strategies, from incorporating expert knowledge to developing targeted data augmentation techniques [44, 52]. These ongoing challenges underscore the critical importance of improving LVLMs’ multimodal comprehension and domain robustness [53, 54].


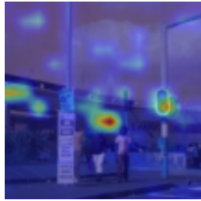
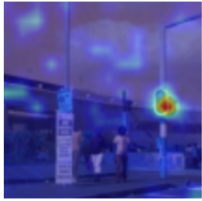

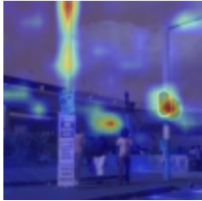
 <p>Q: Please describe what's in the picture?</p>	<p>Original</p>  <p>y_{lose}: Several people walking on the road.</p>	<p>Contrast</p>  <p>y_1: Red traffic light on the roadside.</p>	<p>Crop</p>  <p>y_2: Billboard on the roadside people.</p>	<p>Diffusion-W</p>  <p>y_3: Lamps light the roadside people.</p>
	<p>y_{win}: Several people walking on the road with a red traffic light and a billboard on roadside.</p>			

Figure 2. The winner answer y_{win} through attention visualization indicates how SHAPE enables holistic caption generation. And y_{lose} is the original generation. The green text represents correctly recognized content, while the red text represents incorrect recognition.

2.2. Data Augmentation in LVLMs

While data augmentation has proven successful in computer vision tasks, its application to LVLMs reveals unexpected challenges and insights [7, 14, 16, 58]. Recent studies show that LVLMs exhibit remarkable sensitivity to minor image perturbations—even simple transformations like random flipping can induce significant semantic shifts in model outputs. This behavior, distinctly different from traditional computer vision models’ robustness to augmentation, suggests fundamental differences in how LVLMs process and interpret visual information. Standard augmentation strategies from contrastive learning often lead to inconsistent model behaviors rather than improved robustness.

Intriguingly, this sensitivity to visual perturbations has emerged as a valuable property for model improvement [2, 9, 50, 51]. The semantic divergence between outputs from original and augmented inputs creates informative preference pairs, offering a novel approach to model alignment without extensive manual annotation.

2.3. LVLMs Preference Alignment

Aligning LVLm outputs with human preferences remains a critical challenge, primarily due to the independent pre-training of visual and language modalities. While conventional methods like PPO and DPO have demonstrated effectiveness in language models [22, 33, 35], their application to multimodal scenarios faces key limitations: they require costly human preference data, depend heavily on external AI feedback, and often overlook models’ inherent capabilities.

These challenges are amplified in multimodal contexts, where precise visual-linguistic alignment is crucial. Current approaches largely overlook intrinsic LVLm characteristics, particularly their sensitivity to visual perturbations [12, 40, 46], which could serve as valuable alignment signals. Although recent work has begun exploring model-inherent properties, the potential of leveraging visual sensitivity for

preference pair generation remains untapped. This gap motivates the development of efficient, model-specific alignment strategies that can fully utilize these unique characteristics.

3. Method

Motivation. Inspired by these observations detailed in Figure 2 and Table 3, our motivation lies in transforming what was once considered a limitation—the model’s susceptibility to input variations—into an opportunity. We leverage these variations as an automated supervision mechanism, thus optimizing alignment processes, promoting semantic richness, and maintaining low annotation costs while enhancing the comprehensive understanding capabilities of LVLMs.

We present SHAPE, a framework that transforms standard supervised text-image pairs into more holistic preference triplets for LVLm alignment. Instead of relying on costly preference annotations, our approach leverages existing supervised data to construct competitive preference pairs for efficient self-supervised preference learning. As shown in Figure 3, SHAPE extends beyond traditional SFT (Figure 3(a)) and simple augmentation methods like SeVa (Figure 3(b)), by implementing multiple image augmentations to generate diverse perspectives that are synthesized into more comprehensive outputs (Figure 3(c)).

Preference Optimization. Preference optimization has shown promise in fine-tuning language models and aligning their behavior with desired outcomes. Given an input prompt x , a language model with policy π_θ can produce a conditional distribution:

$$\pi_\theta(y|x) \leftarrow \prod_{k=1}^L \pi_\theta(y_k|y_{<k}, x),$$

where $y_{<k}$ represents the generated token before the current prediction y_k , and L is the length of the token sequence.

The preference data is defined as $\mathcal{D} = \{(x^i, y_w^i, y_l^i)\}_{i=1}^N$, where y_w^i denotes the preferred response for the input prompt x^i , and y_l^i denotes the dispreferred one. Taking DPO [33]

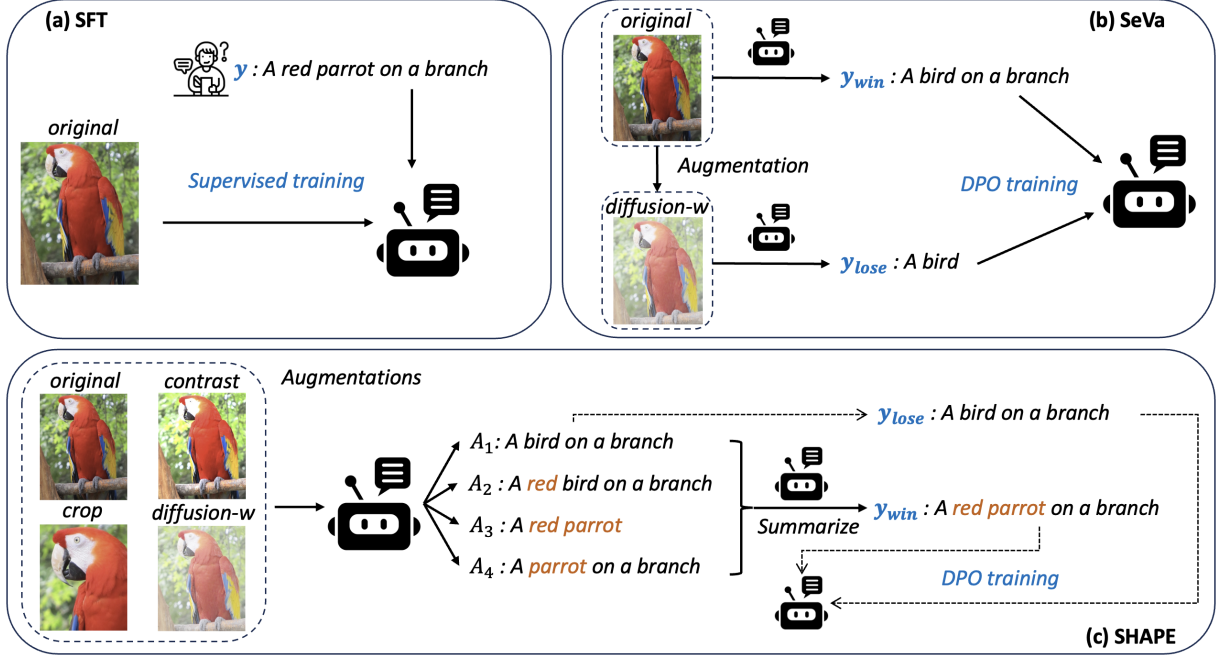


Figure 3. Overview of SHAPE: Unlike traditional SFT, which relies on single-path supervised learning with human preference intervention (e.g., (a) SFT), or simple augmentation methods (e.g., (b) SeVa), SHAPE fully leverages the potential of LVLMs by extending the self-supervised optimization paradigm to Visual Question Answering (VQA). It enriches image-side understanding to generate holistic training signals, enabling more reliable and detailed visual comprehension without requiring additional annotations.

as a representative example, it formulates the probability of obtaining each preference pair as a Bradley-Terry (BT) preference model:

$$p(y_w \succ y_l | x) = \frac{\exp(r(x, y_w))}{\exp(r(x, y_w)) + \exp(r(x, y_l))},$$

where $r(x, y)$ represents the reward or quality score for answer y given input x . This formulation naturally captures our intuition that the winning answer should have a higher probability of being preferred, while maintaining a meaningful comparison with the competitive loser. DPO optimizes the language models with the following loss:

$$\mathcal{L}(\pi_\theta; \pi_{\text{ref}}) = -\mathbb{E}_{\mathcal{D}} \log \sigma \left(\beta \log \frac{\pi_\theta(y_w | x)}{\pi_{\text{ref}}(y_w | x)} - \beta \log \frac{\pi_\theta(y_l | x)}{\pi_{\text{ref}}(y_l | x)} \right),$$

Self-supervised Preference Optimization. In SeVa [60], they construct the preference dataset with the original image’s output as the winner choice and the augmented image’s output as the loser choice:

$$\begin{aligned} y_w &\leftarrow \pi_\theta(\cdot | x), \\ y_l &\leftarrow \pi_\theta(\cdot | f(x)), \end{aligned}$$

where x is the input of LVLMs, i.e. the question concatenated with image. $f(\cdot)$ is the data augmentation method, i.e. diffusion noise augmentation.

We note that for the same image, the output of model reasoning is different when different image-augmented methods are used. Although they may focus on fewer details, the diversity is improved. Figure 2 shows how the attention patterns of LVLMs change with different data augmentation methods, resulting in a broader range of candidate outputs. Based on this observation, We can summarize the outputs of different image-augmented methods as the winner choice and set the origin output as loser choice:

$$\begin{aligned} y_l &\leftarrow \pi_\theta(\cdot | x), \\ y^i &\leftarrow \pi_\theta(\cdot | f_i(x)), \quad i \in [1, \dots, M] \\ y_w &\leftarrow \pi_\theta(\cdot | y^1 || y^2 || \dots || y^M || p), \end{aligned}$$

where p is the summarization prompt, such as “Please provide a comprehensive summary based on the following candidate answers.”

After obtaining the preference data, we fine-tune the aligned visual model using DPO. For each iteration t , we use the last iteration fine-tuned model $\pi_{\theta_{t-1}}$ as the reference model. Then the loss at iteration t is:

$$\mathcal{L}_t = -\mathbb{E}_{\mathcal{D}} \log \sigma \left(\beta \log \frac{\pi_{\theta_t}(y_w | x)}{\pi_{\theta_{t-1}}(y_w | x)} - \beta \log \frac{\pi_{\theta_t}(y_l | x)}{\pi_{\theta_{t-1}}(y_l | x)} \right).$$

We provide the workflow of SHAPE in Algorithm 1. The procedure iteratively refines the visual language model through self-supervised preference optimization.

Model	MMVet							MMBench		POPE			
	All	rec	ocr	know	gen	spat	math	en	cn	All	rand	pop	adv
LLaVA-1.5-7B	30.5	35.7	21.9	17.7	19.7	24.7	7.7	64.3	58.3	85.9	89.5	86.7	81.7
+ CSR	33.9	39.2	23.3	21.9	24.5	27.7	7.7	65.5	59.4	86.8	89.4	87.4	83.6
+ SeVa	37.2	40.2	29.9	21.8	23.9	34.3	7.7	65.6	59.2	86.7	89.4	87.1	83.6
+ SHAPE	41.8	46.1	33.8	32.5	37.0	39.2	7.7	65.7	59.4	93.9	95.5	95.2	91.0
LLaVA-1.5-13B	35.4	38.9	32.2	23.3	24.8	29.7	24.8	67.7	63.6	85.9	89.6	86.5	82.0
+ CSR	37.8	41.0	32.5	24.6	30.1	32.8	24.8	68.8	64.5	87.3	90.4	89.1	82.2
+ SeVa	41.0	45.4	32.8	32.4	36.7	37.0	25.4	68.7	64.8	87.4	90.5	89.0	82.7
+ SHAPE	42.8	46.7	37.7	34.6	39.0	39.7	25.0	69.0	65.1	94.5	96.0	95.9	93.3

Table 1. Comparison of SHAPE with state-of-the-art enhancement strategies applied to the LLaVA-1.5-7B (in both 7B and 13B model sizes) across the MMVet, MMBench, and POPE benchmarks.

Algorithm 1 Self-supervised Visual Preference Alignment

Input: Datasets: $\mathcal{D} = \{x^i\}_{i=1}^N$; Initial Model: π_{θ_0} ; Image augmentation methods $\{f_j(\cdot)\}_{j=1}^M$; Iterations: T .

- 1: $\pi_{\text{ref}} \leftarrow \pi_{\theta_0}$ // Initialize the reference model.
- 2: $\mathcal{D}_p = \{\}$ // Initialize the preference dataset.
- 3: **for** $t = 1, \dots, T$ **do**
- 4: **for** each $x^i \in \mathcal{D}$ **do**
- 5: **for** each augmentation methods $f_j(\cdot)$ **do**
- 6: $x_j^i \leftarrow f_j(x^i)$ // Augment images.
- 7: $y_j^i \sim \pi_{\text{ref}}(\cdot|x_j^i)$ // Get candidate answers.
- 8: **end for**
- 9: $y_1^i \leftarrow \pi_{\theta}(\cdot|x^i)$ //Take origin output as loser choice.
- 10: //Summarize candidate answers as winner choice.
- 11: $y_w^i \leftarrow \text{Summarize}(y_1^i, y_2^i, \dots, y_M^i)$
- 12: $\mathcal{D}_p \leftarrow \mathcal{D}_p \cup \{x^i, y_w^i, y_1^i\}$ //Update dataset.
- 13: **end for**
- 14: $\pi_{\theta_t} \leftarrow \text{argmin}_{\theta} \mathcal{L}_t(\pi_{\theta_t}, \pi_{\text{ref}})$ //Update target model.
- 15: $\pi_{\text{ref}} \leftarrow \pi_{\theta_t}$ //Update reference model.
- 16: **end for**

Output: Aligned visual model π_{θ_T} .

4. Experiment

4.1. Settings

Data construction. The source data are obtained from the LLaVA665k SFT dataset [27]. Specifically, image-question pairs from TextVQA [37] and OCRVQA [31] (collectively referred to as “text+ocr”) within LLaVA665k are used to generate the DPO preference data.

Training Strategies. Following the settings of prior work [27, 55], we take CLIP-VIT-L-336px as vision encoder, the batch size is 128, and the learning rate is $2e^{-6}$. The default LoRA rank r is set to 1024 and the scale parameter β in DPO is fixed at 0.1.

Evaluation Benchmarks. We evaluate SHAPE across three categories of benchmarks: comprehensive benchmarks, general VQA and hallucination benchmarks. There includes: (1) Comprehensive benchmarks(MM-Vet [49], MMBench [29], MME [48], SEED [21], LLaVA-Bench [28]); (2)General VQA (ScienceQA [30], GQA [18], VisWiz [15]); (3) Hallucination benchmark(POPE [24], CHAIR [34]) . More detailed descriptions are provided in Appendix 6.1.

Data Augment Impact. After an extensive exploration of data augmentation strategies and careful consideration of summary elements, we chose a combination of three augmentation strategies along with the original image. We evaluated various data augmentation combinations to optimize self-supervised training process of SHAPE for LVLMS. Based on comprehensive comparative experiments in Table 3, we identified an optimal set of augmentation strategies, focusing on transformations in three key dimensions of the image: contrast, noise, and spatial region. These selected strategies were integrated into the training pipeline of SHAPE to maximize data diversity.

A critical enhancement to our method was the addition of a response summarization step. By consolidating multiple augmentation-generated perspectives into a cohesive response, this step bridges the gap between diverse individual outputs and comprehensive understanding. This approach forms the foundation for our experimental design in the subsequent ablation studies.

4.2. Comparison with State of the Art

To comprehensively evaluate the effectiveness of our proposed alignment strategy, we compare SHAPE against several SOTA models, including LLaVA-1.5, CSR, and SeVa. The results indicate that SHAPE consistently outperforms these baselines across a range of evaluation benchmarks, demonstrating its superior ability in preference alignment, robustness, and task-specific capabilities.

Model	MME ^P	MME ^C	SEED	LLaVA ^W	SQA	GQA	VisWiz	CHAIR _s ↓	CHAIR _i ↓
LLaVA-1.5-7B	1510.7	348.2	58.6	63.4	66.8	62.0	50.0	48.8	14.9
+ CSR	1524.2	367.9	60.3	71.1	70.7	62.3	54.1	21.0	6.0
+ SeVa	1531.0	369.2	65.8	72.2	67.5	60.7	51.5	20.5	5.8
+ SHAPE	1539.2	370.0	67.4	73.1	71.5	62.8	55.3	19.5	5.4
LLaVA-1.5-13B	1531.3	295.4	61.6	70.7	71.6	63.3	53.6	48.3	14.1
+ CSR	1530.6	303.9	62.9	74.7	75.1	63.7	56.8	28.0	7.3
+ SeVa	1533.9	305.1	68.6	80.1	71.2	63.4	54.7	23.6	6.5
+ SHAPE	1544.0	306.9	69.3	82.5	72.5	64.4	55.8	23.1	6.6

Table 2. Comparison of SHAPE with state-of-the-art enhancement strategies applied to the LLaVA-1.5-7B across various evaluation benchmarks. SHAPE achieved the best scores on most tasks. In the CHAIR tasks, where lower scores are better, SHAPE also showed better performance, indicating that it effectively improved the overall performance of the model.

We selected these baselines for their distinct approaches to preference alignment in LVLMs, which have been pivotal in advancing large vision-language models without relying heavily on manually labeled data. Specifically, LLaVA-1.5 serves as a foundational baseline that lacks advanced alignment techniques, providing a point of reference for evaluating the value added by different alignment strategies. CSR utilizes a reward-based calibration mechanism, attempting to form preference pairs through a self-reinforcing feedback loop that effectively reduces the reliance on annotated datasets. SeVa implements DPO but primarily compares raw and enhanced outputs, limiting its capacity for capturing semantic nuances. These diverse strategies provide a comprehensive backdrop for analyzing the advantages brought by SHAPE, particularly in leveraging unsupervised data to align model outputs effectively and overcome the existing limitations in preference alignment.

SHAPE Bootstraps LLM’s Performance. The results in Table 1 and Table 2 illustrate that SHAPE consistently outperforms baseline models across multiple benchmarks, highlighting its strengths in various vision-language tasks.

Across MMVet and MMBench (shown in Table 1), SHAPE achieved superior overall scores regardless of model size. In the 7B setting, it attains an “All” score of 41.8 on MMVet, surpassing SeVa (37.2) and CSR (33.9). This trend continues in the 13B setting, where SHAPE maintains its lead with an “All” score of 42.8. The consistently better performance across different scales suggests that the proposed alignment strategy is not only effective but also scalable, offering robust enhancements to the model’s comprehension abilities as capacity increases.

Task-specific analysis reveals strengths in knowledge-based and generative tasks, with our method achieving scores of 34.6 and 39.0 on MMVet’s respective subtasks in the 13B setting, surpassing all baselines including in general VQA evaluations. The approach demonstrates improved accuracy and reduced hallucinations as evidenced by POPE and CHAIR evaluations, suggesting it effectively addresses

current alignment limitations across diverse vision-language tasks while generating more informative and contextually appropriate responses.

Why SHAPE Better. Figure 4 presents a comparative evaluation of SHAPE, SeVa, CSR, and LLaVA-1.5-7B/13B models on the MMVet benchmark, with GPT-4V serving as the judge. This analysis examines two key metrics: pairwise win rates and average response length. The GPT-4V evaluation offers insights into each model’s effectiveness in visual-language tasks. For details on GPT-4V-assisted preference annotation, refer to Appendix 6.4.

Win rate analysis suggests that SHAPE generates more informative responses than LLaVA-1.5, CSR, and SeVa across both 7B and 13B variants. On average, it produces 57-token responses in the 7B configuration and 72 tokens in the 13B configuration, whereas other models generate shorter outputs. These findings align with prior research [36, 38, 57], which associates longer responses with improved multimodal comprehension. This trend is more pronounced in larger models, potentially explaining SHAPE’s increased win rate against SeVa from 72% to 88% when scaling from 7B to 13B. Qualitative comparisons are available in Appendix 6.3.

4.3. Ablation Study

To gain deeper insights into the effectiveness of SHAPE in aligning LVLMs, we conduct ablation studies to isolate the impact of key components, including data augmentation, summarization, and architectural parameters, identifying the optimal configuration.

Data Augmentation Strategies. Building on our framework from paragraph 4.1, we conducted detailed experiments to quantify the impact of specific augmentation combinations. We evaluated both individual augmentation strategies and their combinations to identify the most effective configuration, assessing performance on MMVet, MMBench, and POPE benchmarks.

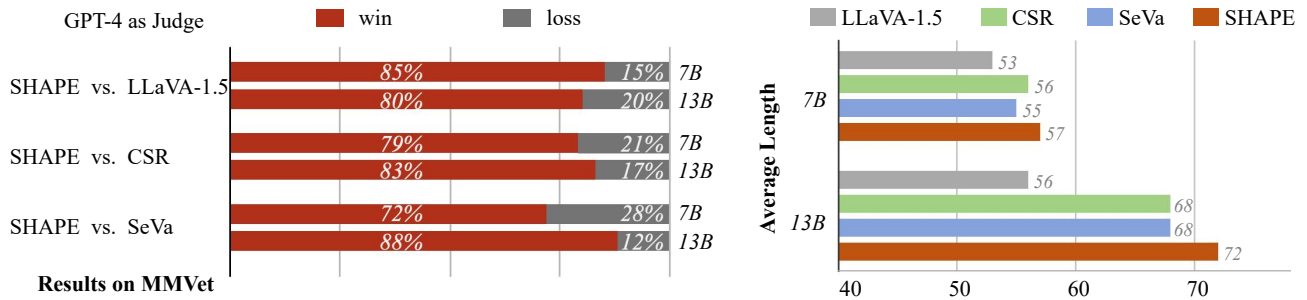


Figure 4. Evaluation of SHAPE, SeVa, CSR, and LLaVA-1.5 (7B and 13B) on MMVet, comparing win rates and average output lengths, with GPT-4 as the judge for visual-language task performance.

Experimental results indicate that moderate augmentation strength yields the best performance, as both overly strong and excessively weak augmentations negatively affect DPO training. Based on the experimental results and the suitability of the augmentation strength as detailed in Appendix 6.2, we finally selected candidate-3 (Contrast + Diffusion-W + Gamma) as our augmentation scheme, wherein each augmentation was applied to distort images (along with the questions) to produce “rejected” responses, paired with “chosen” responses from the original image input. This approach enabled the creation of high-quality preference pairs, subsequently used to guide the DPO training process.

Evaluation results further confirmed the benefits of these augmentation strategies for multimodal comprehension, helping the model more clearly distinguish between “chosen” and “rejected” responses. The progressive strategy combination analysis reveals the importance of strategic integration, as shown in Table 3. While individual augmentations provide modest gains, their combination yields substantially stronger results. Specifically, the candidate-3 configuration provided the optimal balance between performance gains and complexity. Integrating multiple strategy combinations significantly enhanced the extraction of local detail features, resulting in superior summarization capabilities.

Impact with Summary Module. SHAPE enhances preference alignment through its advanced summarization capability, generating richer and more context-aware summaries. To assess the impact of this summarization functionality, we compare SHAPE with SeVa, a model with a similar architecture but without the summarization feature. As shown in Table 4, while SeVa achieves competitive results, with a score of 37.2 on MMVet and 65.6 on MMB (using 16k dataset scale), SHAPE consistently outperforms it, achieving 41.8 on MMVet and 65.7 on MMB with the same data scale. This clearly demonstrates that the summarization feature in SHAPE significantly improves alignment quality and overall model comprehension.

The analysis further examined three specific summary

Method	MMVet	MMB	POPE
LLaVA-1.5-7B	30.5	64.3	85.9
+ RandFlip	33.7	64.4	86.7
+ Contrast	35.6	65.1	86.7
+ Crop(0-20%)	35.0	64.5	86.1
+ Diffusion-S	34.6	65.2	86.6
+ Diffusion-W	37.2	65.6	89.4
+ Gamma	37.0	65.2	89.2
SHAPE			
+ Candidate-1	38.7	65.2	87.4
+ Candidate-2	41.4	65.4	89.4
+ Candidate-3	41.7	65.7	92.7
+ Candidate-4	41.8	65.9	93.6

Table 3. Comparison of augmentation strategies to identify the best-performing schemes on MMVet, MMB and POPE. The top section shows individual augmentation results, the middle section shows performance with varying numbers of combined strategies, and the bottom section shows results with different summary combinations. And SeVa strategies use Diffusion-W on the LLaVA-1.5-7B.

configurations: summary-1 (Contrast + Diffusion-W + Gamma), summary-2 (Crop + Diffusion-S + Gamma), and summary-3 (RandFlip + Diffusion-S + Diffusion-W). Table 3 shows summary-1 performed best on MMVet and POPE, while summary-2 slightly outperformed on MMB. These results indicate that different augmentation combinations offer varying benefits across benchmarks, with the optimal configuration depending on the specific characteristics of the target task. The summarization mechanism provides more nuanced guidance during preference optimization, enabling SHAPE to excel in tasks requiring deep contextual understanding.

Impact with Target Answers. To assess the advantage of SHAPE’s unsupervised alignment strategy, we compare it with SFT using subsets of LLaVA665k—specifically 15k (2%), 66k (10%), and 132k (20%) instances. Similar to SeVa, SHAPE significantly reduces dependency on labeled data while still achieving superior performance. SHAPE reaches

Method	Scale	MMVet	MMB	POPE
LLaVA-1.5	-	30.5	64.3	85.9
- SFT(10%)	66k	32.8	64.9	86.0
- SFT(20%)	66k	33.9	64.2	86.1
- SFT	102k	32.5	65.2	86.7
SeVa	8k	34.8	65.3	86.2
SeVa	16k	37.2	65.6	86.7
SHAPE	8k	36.5	65.5	90.3
SHAPE	16k	41.8	65.7	93.6

Table 4. Comparison of SFT, SeVa, and SHAPE on LLaVA-1.5-7B across MMVet, MMB, and POPE benchmarks. SFT uses subsets of LLaVA665k (15k, 66k, and 102k samples), while SeVa and SHAPE rely on unsupervised data without ground truth annotations. SHAPE achieves superior performance with smaller data subsets and reduced training costs, highlighting its efficiency.

LoRA r	Method	MMVet	MMB	POPE
-	LLaVA-1.5	30.7	64.3	85.9
256	SeVa	34.0	65.1	86.6
	SHAPE	38.7	64.9	91.0
512	SeVa	35.5	65.5	86.8
	SHAPE	41.2	65.6	93.2
1024	SeVa	37.2	65.6	86.7
	SHAPE	41.8	65.7	93.6
2048	SeVa	33.5	65.0	84.5
	SHAPE	40.5	65.2	93.0

Table 5. Performance comparison across LoRA [17] rank r from 256 to 2048. SHAPE achieves consistently strong results, with optimal performance at $r=1024$.

a score of 41.8 on MMVet using only 16k unsupervised samples, surpassing SFT performance even when using larger labeled datasets of up to 132k instances, as detailed in Table 4. This highlights the effectiveness of SHAPE’s unsupervised preference optimization, which not only minimizes reliance on costly annotations but also delivers higher performance with significantly less data and training effort.

the performance of SFT even with larger labeled datasets, outperforming SFT even when larger labeled datasets are used, as detailed in Table 4.

Impact of LoRA Module. To investigate the influence of the LoRA adaptation module, we conducted an ablation study with varying low-rank hyper-parameters across three multimodal comprehension benchmarks, as shown in Table 5. The parameter choice is crucial because it determines how much new knowledge the model can effectively absorb during fine-tuning. We found that increasing the rank r generally boosts performance on downstream tasks, suggesting that a higher rank allows the model to capture more

knowledge. However, further increasing r to 2048 triggered performance degradation (40.5 on MMVet, 65.2 on MMB), consistent with catastrophic forgetting during the training of the LLM [13]. Consequently, SHAPE adopted $r=1024$ to achieve the best trade-off, with the delta importance factor α consistently set at twice the value of r , ensuring a stable and effective fine-tuning process.

Method	Offline (h)	Training (h)	Total (h)	MMVet
SeVa	0.05	3.50	3.55	37.2
SHAPE	0.21	3.50	3.71	42.8

Table 6. Training cost/result of LLaVA-1.5-7B on 16k samples.

Trade-off between training cost and efficiency. While SHAPE necessitates additional computational resources for offline data generation, although these constitute a modest proportion of the total duration of training. Table 6 shows the self-augmented training results of LLaVA-1.5-7B on 4 A100 GPUs with 16k training data (8k TextVQA + 8k OCRVQA). SHAPE only has 9 min more offline time than SeVa, but it brings a 5.6% improvement to MMVet. Overall, the trade-off in time for offline data augmentation is worthwhile.

5. Conclusion

In this paper, we have proposed SHAPE, a self-supervised framework tailored for Large Visual Language Models to achieve more effective preference alignment without the need for human preference annotations. SHAPE has achieved this by transforming off-the-shelf text-image pairs datasets into preference data, where each preference triplet consists of a winner text that consistently improves in holistness and outperforms the loser text in quality, thereby pushing the model to progressively enhance the alignment performance throughout preference finetuning. The extensive experiments have demonstrated that SHAPE significantly enhances performance across multiple benchmarks, showing consistent gains for both 7B and 13B model sizes. Our qualitative analysis has further highlighted that LVLMs yielded from SHAPE exhibit enhanced attention to visual details and provide richer, contextually aware responses aligned with human preferences.

Limitations and Future Works. SHAPE still relies on a predefined strategy for visual augmentations, which may limit the diversity of transformations. Additionally, we plan to investigate automated prompt generation and refinement to better adapt to different data distributions, thereby improving the quality of the text summarization step, which is currently designed manually. Further validation across diverse real-world tasks is also required to assess generalizability more comprehensively.

References

- [1] Jean-Baptiste Alayrac, Jeff Donahue, Pauline Luc, Antoine Miech, Iain Barr, Yana Hasson, Karel Lenc, Arthur Mensch, Katherine Millican, Malcolm Reynolds, et al. Flamingo: a visual language model for few-shot learning. *Advances in neural information processing systems*, 35:23716–23736, 2022. 1
- [2] Muhammad Awais, Muzammal Naseer, Salman Khan, Rao Muhammad Anwer, Hisham Cholakkal, Mubarak Shah, Ming-Hsuan Yang, and Fahad Shahbaz Khan. Foundation models defining a new era in vision: a survey and outlook. *IEEE Transactions on Pattern Analysis and Machine Intelligence*, 2025. 3
- [3] Yuntao Bai, Andy Jones, Kamal Ndousse, Amanda Askell, Anna Chen, Nova DasSarma, Dawn Drain, Stanislav Fort, Deep Ganguli, Tom Henighan, et al. Training a helpful and harmless assistant with reinforcement learning from human feedback. *arXiv preprint arXiv:2204.05862*, 2022. 1, 13
- [4] Pratyay Banerjee, Tejas Gokhale, Yezhou Yang, and Chitta Baral. Weaqa: Weak supervision via captions for visual question answering. *arXiv preprint arXiv:2012.02356*, 2020. 1
- [5] Soravit Changpinyo, Doron Kukliansky, Idan Szpektor, Xi Chen, Nan Ding, and Radu Soricut. All you may need for vqa are image captions. *arXiv preprint arXiv:2205.01883*, 2022. 1
- [6] Lin Chen, Jinsong Li, Xiaoyi Dong, Pan Zhang, Conghui He, Jiaqi Wang, Feng Zhao, and Dahua Lin. Sharegpt4v: Improving large multi-modal models with better captions. *arXiv preprint arXiv:2311.12793*, 2023. 1
- [7] Ting Chen, Simon Kornblith, Mohammad Norouzi, and Geoffrey Hinton. A simple framework for contrastive learning of visual representations. In *International conference on machine learning*, pages 1597–1607. PMLR, 2020. 3, 13
- [8] Xi Chen, Josip Djolonga, Piotr Padlewski, Basil Mustafa, Soravit Changpinyo, Jialin Wu, Carlos Riquelme Ruiz, Sebastian Goodman, Xiao Wang, Yi Tay, et al. Pali-x: On scaling up a multilingual vision and language model. *arXiv preprint arXiv:2305.18565*, 2023. 2
- [9] Zixiang Chen, Yihe Deng, Huizhuo Yuan, Kaixuan Ji, and Quanquan Gu. Self-play fine-tuning converts weak language models to strong language models. *arXiv preprint arXiv:2401.01335*, 2024. 3
- [10] Ganqu Cui, Lifan Yuan, Ning Ding, Guanming Yao, Wei Zhu, Yuan Ni, Guotong Xie, Zhiyuan Liu, and Maosong Sun. Ultrafeedback: Boosting language models with high-quality feedback. *arXiv preprint arXiv:2310.01377*, 2023. 13
- [11] Wenliang Dai, Junnan Li, Dongxu Li, Anthony Tiong, Junqi Zhao, Weisheng Wang, Boyang Li, Pascale Fung, and Steven Hoi. InstructBLIP: Towards general-purpose vision-language models with instruction tuning. In *Thirty-seventh Conference on Neural Information Processing Systems*, 2023. 2
- [12] Haiwen Diao, Yufeng Cui, Xiaotong Li, Yuezhe Wang, Huchuan Lu, and Xinlong Wang. Unveiling encoder-free vision-language models. *Advances in Neural Information Processing Systems*, 37:52545–52567, 2025. 3
- [13] Minghao Fu, Ke Zhu, and Jianxin Wu. Dtl: Disentangled transfer learning for visual recognition. In *Proceedings of the AAAI Conference on Artificial Intelligence*, pages 12082–12090, 2024. 8
- [14] Jean-Bastien Grill, Florian Strub, Florent Altché, Corentin Tallec, Pierre Richemond, Elena Buchatskaya, Carl Doersch, Bernardo Avila Pires, Zhaohan Guo, Mohammad Gheshlaghi Azar, et al. Bootstrap your own latent—a new approach to self-supervised learning. *Advances in neural information processing systems*, 33:21271–21284, 2020. 3, 13
- [15] Danna Gurari, Qing Li, Abigale J Stangl, Anhong Guo, Chi Lin, Kristen Grauman, Jiebo Luo, and Jeffrey P Bigham. Vizwiz grand challenge: Answering visual questions from blind people. In *Proceedings of the IEEE conference on computer vision and pattern recognition*, pages 3608–3617, 2018. 5, 12
- [16] Kaiming He, Haoqi Fan, Yuxin Wu, Saining Xie, and Ross Girshick. Momentum contrast for unsupervised visual representation learning. In *Proceedings of the IEEE/CVF conference on computer vision and pattern recognition*, pages 9729–9738, 2020. 2, 3, 13
- [17] Edward J Hu, Yelong Shen, Phillip Wallis, Zeyuan Allen-Zhu, Yuanzhi Li, Shean Wang, Lu Wang, and Weizhu Chen. Lora: Low-rank adaptation of large language models. *arXiv preprint arXiv:2106.09685*, 2021. 8
- [18] Drew A Hudson and Christopher D Manning. Gqa: A new dataset for real-world visual reasoning and compositional question answering. In *Proceedings of the IEEE/CVF conference on computer vision and pattern recognition*, pages 6700–6709, 2019. 5, 12
- [19] Dongfu Jiang, Xiang Ren, and Bill Yuchen Lin. Llm-blender: Ensembling large language models with pairwise ranking and generative fusion. *arXiv preprint arXiv:2306.02561*, 2023. 1
- [20] Harrison Lee, Samrat Phatale, Hassan Mansoor, Thomas Mesnard, Johan Ferret, Kellie Lu, Colton Bishop, Ethan Hall, Victor Carbune, Abhinav Rastogi, et al. Rlaif: Scaling reinforcement learning from human feedback with ai feedback. *arXiv preprint arXiv:2309.00267*, 2023. 2, 13
- [21] Bohao Li, Rui Wang, Guangzhi Wang, Yuying Ge, Yixiao Ge, and Ying Shan. Seed-bench: Benchmarking multimodal llms with generative comprehension. *arXiv preprint arXiv:2307.16125*, 2023. 5, 12
- [22] Baiqi Li, Zhiqiu Lin, Wenxuan Peng, Jean de Dieu Nyandwi, Daniel Jiang, Zixian Ma, Simran Khanuja, Ranjay Krishna, Graham Neubig, and Deva Ramanan. Naturalbench: Evaluating vision-language models on natural adversarial samples. *Advances in Neural Information Processing Systems*, 37:17044–17068, 2025. 3
- [23] Junnan Li, Dongxu Li, Caimeing Xiong, and Steven Hoi. Blip: Bootstrapping language-image pre-training for unified vision-language understanding and generation. In *International conference on machine learning*, pages 12888–12900. PMLR, 2022. 2
- [24] Yifan Li, Yifan Du, Kun Zhou, Jinpeng Wang, Wayne Xin Zhao, and Ji-Rong Wen. Evaluating object hallucination in large vision-language models. *arXiv preprint arXiv:2305.10355*, 2023. 5, 12

- [25] Yanwei Li, Chengyao Wang, and Jiaya Jia. Llama-vid: An image is worth 2 tokens in large language models. In *European Conference on Computer Vision*, pages 323–340. Springer, 2025. 1
- [26] Tsung-Yi Lin, Michael Maire, Serge Belongie, James Hays, Pietro Perona, Deva Ramanan, Piotr Dollár, and C Lawrence Zitnick. Microsoft coco: Common objects in context. In *Computer Vision—ECCV 2014: 13th European Conference, Zurich, Switzerland, September 6–12, 2014, Proceedings, Part V 13*, pages 740–755. Springer, 2014. 12
- [27] Haotian Liu, Chunyuan Li, Yuheng Li, and Yong Jae Lee. Improved baselines with visual instruction tuning. In *Proceedings of the IEEE/CVF Conference on Computer Vision and Pattern Recognition*, pages 26296–26306, 2024. 1, 5
- [28] Haotian Liu, Chunyuan Li, Qingyang Wu, and Yong Jae Lee. Visual instruction tuning. *Advances in neural information processing systems*, 36, 2024. 1, 2, 5, 12
- [29] Yuan Liu, Haodong Duan, Yuanhan Zhang, Bo Li, Songyang Zhang, Wangbo Zhao, Yike Yuan, Jiaqi Wang, Conghui He, Ziwei Liu, et al. Mmbench: Is your multi-modal model an all-around player? In *European Conference on Computer Vision*, pages 216–233. Springer, 2025. 5, 12
- [30] Pan Lu, Swaroop Mishra, Tanglin Xia, Liang Qiu, Kai-Wei Chang, Song-Chun Zhu, Oyvind Tafjord, Peter Clark, and Ashwin Kalyan. Learn to explain: Multimodal reasoning via thought chains for science question answering. *Advances in Neural Information Processing Systems*, 35:2507–2521, 2022. 5, 12
- [31] Anand Mishra, Shashank Shekhar, Ajeet Kumar Singh, and Anirban Chakraborty. Ocr-vqa: Visual question answering by reading text in images. In *2019 international conference on document analysis and recognition (ICDAR)*, pages 947–952. IEEE, 2019. 5
- [32] Zhiliang Peng, Wenhui Wang, Li Dong, Yaru Hao, Shaohan Huang, Shuming Ma, and Furu Wei. Kosmos-2: Grounding multimodal large language models to the world. *arXiv preprint arXiv:2306.14824*, 2023. 2
- [33] Rafael Rafailov, Archit Sharma, Eric Mitchell, Christopher D Manning, Stefano Ermon, and Chelsea Finn. Direct preference optimization: Your language model is secretly a reward model. *Advances in Neural Information Processing Systems*, 36, 2024. 3
- [34] Anna Rohrbach, Lisa Anne Hendricks, Kaylee Burns, Trevor Darrell, and Kate Saenko. Object hallucination in image captioning. *arXiv preprint arXiv:1809.02156*, 2018. 5, 12
- [35] John Schulman, Filip Wolski, Prafulla Dhariwal, Alec Radford, and Oleg Klimov. Proximal policy optimization algorithms. *arXiv preprint arXiv:1707.06347*, 2017. 3
- [36] Dongjae Shin, HyeonSeok Lim, Inho Won, Changsu Choi, Minjun Kim, Seungwoo Song, Hangeol Yoo, Sangmin Kim, and Kyungtae Lim. X-llava: Optimizing bilingual large vision-language alignment. *arXiv preprint arXiv:2403.11399*, 2024. 6
- [37] Amanpreet Singh, Vivek Natarajan, Meet Shah, Yu Jiang, Xinlei Chen, Dhruv Batra, Devi Parikh, and Marcus Rohrbach. Towards vqa models that can read. In *Proceedings of the IEEE/CVF conference on computer vision and pattern recognition*, pages 8317–8326, 2019. 5
- [38] Guohao Sun, Can Qin, Jiamian Wang, Zeyuan Chen, Ran Xu, and Zhiqiang Tao. Sq-llava: Self-questioning for large vision-language assistant. In *European Conference on Computer Vision*, pages 156–172. Springer, 2024. 6
- [39] Zhiqing Sun, Sheng Shen, Shengcao Cao, Haotian Liu, Chunyuan Li, Yikang Shen, Chuang Gan, Liang-Yan Gui, Yu-Xiong Wang, Yiming Yang, et al. Aligning large multimodal models with factually augmented rlhf. *arXiv preprint arXiv:2309.14525*, 2023. 1
- [40] Peter Tong, Ellis Brown, Penghao Wu, Sanghyun Woo, Adithya Jairam Vedagiri IYER, Sai Charitha Akula, Shusheng Yang, Jihan Yang, Manoj Middepogu, Ziteng Wang, et al. Cambrian-1: A fully open, vision-centric exploration of multimodal llms. *Advances in Neural Information Processing Systems*, 37:87310–87356, 2025. 3
- [41] Shengbang Tong, Ellis Brown, Penghao Wu, Sanghyun Woo, Manoj Middepogu, Sai Charitha Akula, Jihan Yang, Shusheng Yang, Adithya Iyer, Xichen Pan, et al. Cambrian-1: A fully open, vision-centric exploration of multimodal llms. *arXiv preprint arXiv:2406.16860*, 2024. 13
- [42] Xiyao Wang, Jiuhai Chen, Zhaoyang Wang, Yuhang Zhou, Yiyang Zhou, Huaxiu Yao, Tianyi Zhou, Tom Goldstein, Parminder Bhatia, Furong Huang, et al. Enhancing visual-language modality alignment in large vision language models via self-improvement. *arXiv preprint arXiv:2405.15973*, 2024. 1
- [43] Yue Wu, Zhiqing Sun, Huizhuo Yuan, Kaixuan Ji, Yiming Yang, and Quanquan Gu. Self-play preference optimization for language model alignment. *arXiv preprint arXiv:2405.00675*, 2024. 1
- [44] Tianyi Xiong, Xiyao Wang, Dong Guo, Qinghao Ye, Haoqi Fan, Quanquan Gu, Heng Huang, and Chunyuan Li. Llavacritic: Learning to evaluate multimodal models. *arXiv preprint arXiv:2410.02712*, 2024. 2
- [45] Wei Xiong, Hanze Dong, Chenlu Ye, Ziqi Wang, Han Zhong, Heng Ji, Nan Jiang, and Tong Zhang. Iterative preference learning from human feedback: Bridging theory and practice for rlhf under kl-constraint. In *Forty-first International Conference on Machine Learning*, 2024. 1
- [46] Zhihe Yang, Xufang Luo, Dongqi Han, Yunjian Xu, and Dongsheng Li. Mitigating hallucinations in large vision-language models via dpo: On-policy data hold the key. *arXiv preprint arXiv:2501.09695*, 2025. 3
- [47] Qinghao Ye, Haiyang Xu, Guohai Xu, Jiabo Ye, Ming Yan, Yiyang Zhou, Junyang Wang, Anwen Hu, Pengcheng Shi, Yaya Shi, et al. mplug-owl: Modularization empowers large language models with multimodality. *arXiv preprint arXiv:2304.14178*, 2023. 2
- [48] Shukang Yin, Chaoyou Fu, Sirui Zhao, Ke Li, Xing Sun, Tong Xu, and Enhong Chen. A survey on multimodal large language models. *arXiv preprint arXiv:2306.13549*, 2023. 5, 12
- [49] Weihao Yu, Zhengyuan Yang, Linjie Li, Jianfeng Wang, Kevin Lin, Zicheng Liu, Xinchao Wang, and Lijuan Wang. Mm-vet: Evaluating large multimodal models for integrated capabilities. *arXiv preprint arXiv:2308.02490*, 2023. 5, 12
- [50] Xiaotian Yu, Yang Jiang, Tianqi Shi, Zunlei Feng, Yuexuan Wang, Mingli Song, and Li Sun. How to prevent the continu-

- ous damage of noises to model training? In *Proceedings of the IEEE/CVF Conference on Computer Vision and Pattern Recognition*, pages 12054–12063, 2023. 3
- [51] Weizhe Yuan, Richard Yuanzhe Pang, Kyunghyun Cho, Sainbayar Sukhbaatar, Jing Xu, and Jason Weston. Self-rewarding language models. *arXiv preprint arXiv:2401.10020*, 2024. 1, 3
- [52] Di Zhang, Jingdi Lei, Junxian Li, Xunzhi Wang, Yujie Liu, Zonglin Yang, Jiatong Li, Weida Wang, Suorong Yang, Jianbo Wu, et al. Critic-v: Vlm critics help catch vlm errors in multimodal reasoning. *arXiv preprint arXiv:2411.18203*, 2024. 2
- [53] Pan Zhang, Xiaoyi Dong, Yuhang Zang, Yuhang Cao, Rui Qian, Lin Chen, Qipeng Guo, Haodong Duan, Bin Wang, Linke Ouyang, et al. Internlm-xcomposer-2.5: A versatile large vision language model supporting long-contextual input and output. *arXiv preprint arXiv:2407.03320*, 2024. 2
- [54] Yongting Zhang, Lu Chen, Guodong Zheng, Yifeng Gao, Rui Zheng, Jinlan Fu, Zhenfei Yin, Senjie Jin, Yu Qiao, Xuanjing Huang, et al. Spa-vl: A comprehensive safety preference alignment dataset for vision language model. *arXiv preprint arXiv:2406.12030*, 2024. 2
- [55] Zhiyuan Zhao, Bin Wang, Linke Ouyang, Xiaoyi Dong, Jiaqi Wang, and Conghui He. Beyond hallucinations: Enhancing vlms through hallucination-aware direct preference optimization. *arXiv preprint arXiv:2311.16839*, 2023. 5
- [56] Yiyang Zhou, Zhiyuan Fan, Dongjie Cheng, Sihan Yang, Zhaorun Chen, Chenhang Cui, Xiyao Wang, Yun Li, Linjun Zhang, and Huaxiu Yao. Calibrated self-rewarding vision language models. *Advances in Neural Information Processing Systems*, 2024. 2
- [57] Deyao Zhu, Jun Chen, Xiaoqian Shen, Xiang Li, and Mohamed Elhoseiny. Minigt-4: Enhancing vision-language understanding with advanced large language models. *arXiv preprint arXiv:2304.10592*, 2023. 1, 6
- [58] Ke Zhu, Minghao Fu, and Jianxin Wu. Multi-label self-supervised learning with scene images. In *Proceedings of the IEEE/CVF International Conference on Computer Vision*, pages 6694–6703, 2023. 2, 3
- [59] Ke Zhu, Yin-Yin He, and Jianxin Wu. Coarse is better? a new pipeline towards self-supervised learning with uncurated images. *arXiv preprint arXiv:2306.04244*, 2023.
- [60] Ke Zhu, Liang Zhao, Zheng Ge, and Xiangyu Zhang. Self-supervised visual preference alignment. In *Proceedings of the 32nd ACM International Conference on Multimedia*, pages 291–300, 2024. 2, 4

SHAPE : Self-Improved Visual Preference Alignment by Iteratively Generating Holistic Winner

Supplementary Material

6. Appendix

This appendix provides supplementary details on methodology and experimental procedures. We begin with a description of the evaluation benchmarks 6.1 used to assess model performance. Next, we elaborate on the experimental setup 6.2, including the choice of image augmentation strategies and their impact on model performance. Finally, we present qualitative results 6.3, including visual comparisons and GPT-4V annotations 6.4, which demonstrate the model’s effectiveness in aligning visual and textual information. Source code is publicly available at <https://anonymous.4open.science/r/shape-002C>.

6.1. Evaluation Benchmarks

LLaVA-Bench (In the wild) [28]: A challenging benchmark of 60 diverse tasks designed to evaluate models in naturalistic settings. It specifically tests visual instruction-following and question-answering capabilities in real-world scenarios, offering insights into practical applicability.

MM-Vet [49]: A comprehensive evaluation suite comprising 128 diverse tasks that assess six core visual-language capabilities. This benchmark uniquely combines mathematical reasoning, logical inference, and visual knowledge understanding, providing a rigorous test of multi-modal comprehension.

MM-Bench [29]: A large-scale multi-modal benchmark with 4.7K samples, focusing on visual knowledge and reasoning capabilities. This dataset provides a balanced assessment of both factual knowledge and analytical reasoning in multi-modal contexts.

POPE [24]: A specialized benchmark containing 8,440 samples designed to evaluate model hallucination. It specifically tests models’ ability to provide accurate Yes/No responses about object presence in images, serving as a critical measure of visual grounding reliability.

MME [48]: A benchmark with 14 tasks assessing perception and cognition in LVLMs, challenging interpretative and analytical skills.

SEED [21]: A benchmark designed to evaluate the generative comprehension capabilities of large vision-language models (LVLMs). It includes an extensive dataset of 19K multiple-choice questions with precise human annotations, spanning 12 distinct evaluation dimensions that cover both spatial and temporal understanding across image and video modalities.

ScienceQA [30]: A multimodal benchmark crafted to evaluate and diagnose the multi-hop reasoning abilities and

interpretability of AI systems within the science domain. It features an extensive dataset of approximately 21k multiple-choice questions, spanning a broad spectrum of scientific topics and supplemented with detailed answer annotations, associated lectures, and explanations.

GQA [18]: A dataset specifically engineered for advanced real-world visual reasoning, utilizing scene graph-based structures to generate 22 million diverse, semantically-programmed questions. It incorporates novel evaluation metrics focusing on consistency, grounding, and plausibility, thereby establishing a rigorous standard for vision-language task assessment.

VisWiz [15]: A visual question answering (VQA) dataset derived from naturalistic settings, featuring over 31,000 visual questions. It is distinguished by its goal-oriented approach, with images captured by blind individuals and accompanied by their spoken queries, along with crowdsourced answers.

CHAIR [34]: A well-established benchmark for evaluating object hallucination in image captioning tasks, with two variants: CHAIR_I and CHAIR_S, which assess hallucination at the instance and sentence levels, respectively. We randomly sampled 500 images from the COCO [26] validation set and evaluated object hallucination using the CHAIR metric. Note that a lower CHAIR score indicates fewer hallucinations, which implies better alignment between the captions and the actual content of the images.

$$\text{CHAIR}_I = \frac{\text{Number of hallucinated objects}}{\text{Number of all mentioned objects}},$$

$$\text{CHAIR}_S = \frac{\text{Number of captions with hallucinated objects}}{\text{Number of all captions}}.$$

6.2. Detail of Experimental Setup

Image augmentation strategies. We implement three effective image-side augmentation strategies to generate diverse responses from our model. By applying these techniques to the original images, we produce multiple distinct responses which are then synthesized into a comprehensive final output. This approach enhances model robustness by introducing controlled variations in visual input while maintaining semantic consistency. The augmentation strategies include:

- **Crop**(s_{\min} , s_{\max}): Crop the image from minimum scale to the maximum scale ($s_{\min} = 0.2$, $s_{\max} = 0.5$ in our paper).
- **Diffusion-S (Strong)**: Applies gaussian noise with 500 diffusion steps, creating significant but controlled perturbation.

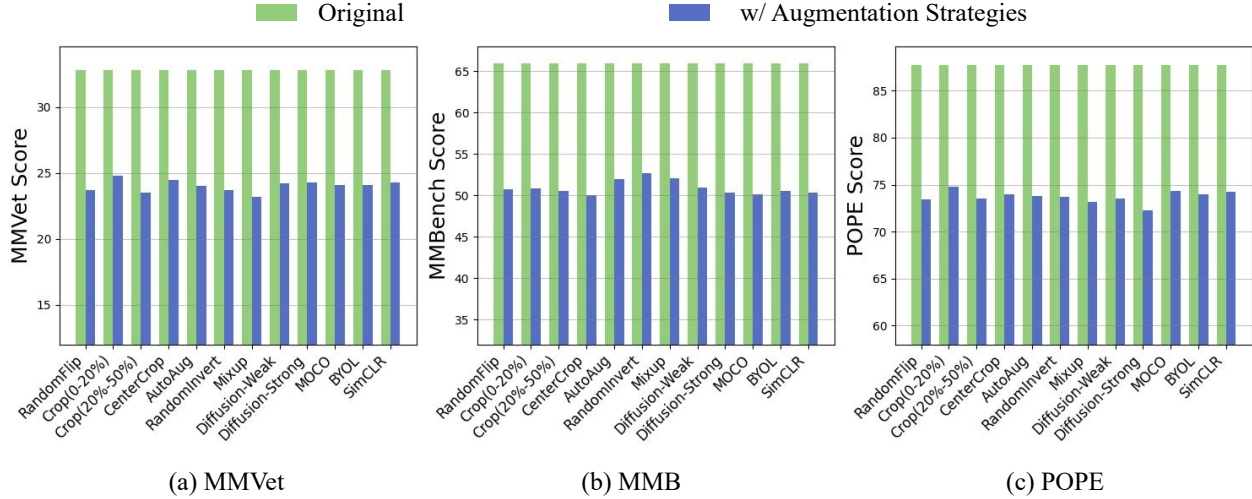


Figure 5. Comparison of 12 data augmentation strategies applied to LLaVA-1.5, including various geometric and color transformations as well as contrast learning enhancement methods. By analyzing these methods, the goal is to find the combination that best improves the performance of LVLMs.

- Diffusion-W (Weak): Introduces gaussian noise with 200 diffusion steps, offering a more moderate level of visual distortion.
- Contrast: Enhances image contrast by a factor of 2, accentuating visual boundaries and feature differences.
- Gamma: Performs gamma correction at a value of 0.8, lightening dark regions in the image. (Note that gamma values above 1 make shadows darker, while values below 1 make dark regions lighter).

Impact with Augmentation Strategies. To better understand how different augmentation strategies influence performance, we conducted comprehensive analysis of 12 widely-used techniques from recent literature [7, 14, 16, 41], as shown in Figure 5. Our investigation revealed important nuances in augmentation effectiveness. Not all augmentation methods provide equal benefits for model performance. Some strategies, particularly strong diffusion noise, proved excessively aggressive and interfered with the model’s ability to extract and learn relevant visual features. Conversely, simpler augmentations like random flipping lacked sufficient complexity to drive meaningful performance improvements. Based on these findings, we carefully selected a combination of three augmentation strategies alongside the original images to strike the perfect balance.

Evaluation of Scalability. To evaluate the scalability of SHAPE, we conducted experiments on the latest releases of DeepSeek-VL2-Tiny (based on DeepSeekMoE-3B) and DeepSeek-VL2 (based on DeepSeekMoE-27B). Table 7 presents quantitative improvements across all evaluation metrics, with more substantial gains observed on larger architectural configurations. When applied to DeepSeek-VL2,

SHAPE elevated MMVet scores from 56.9 to 60.2 and POPE scores from 92.5 to 96.2, indicating that the methodology accommodates scaling to larger architectures and addresses more complex analytical tasks.

Model	MMVet	MMBench	MME	POPE
DeepSeek-VL2-Tiny	52.8	69.2	1,915	88.8
+ SeVa	53.1	70.7	2,086	89.4
+ SHAPE	55.1	73.5	2,103	94.7
DeepSeek-VL2	56.9	79.6	2,253	92.5
+ SeVa	58.5	80.5	2,296	93.8
+ SHAPE	60.2	81.0	2,318	96.2

Table 7. Comparison of SHAPE with sota enhancement strategy applied to the DeepSeek.

6.3. Exhibition Board

This section presents SHAPE is able to process the information in images more accurately, and provide contextually relevant answers in combination with a knowledge base, significantly improving the model’s performance in complex visual-linguistic tasks, which can be seen in Figure 6. This improvement reflects SHAPE’s higher semantic accuracy and stronger reasoning ability in image understanding and text generation tasks.

6.4. GPT-4V-assisted Preference Annotations

GPT-4V’s role as a judge is widely recognized as reliable due to its superior capabilities in visual and linguistic comprehension, enabling a thorough assessment of different models’ performance in multimodal tasks [3, 10, 20]. We present two examples the GPT-4V annotations in the Figure 7 and 8.

Q1: How many gallons of supreme gasoline can I get with \$50?



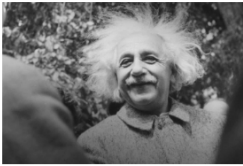
LLaVA-1.5-13B:
Based on the image, you can get 3.6 gallons of supreme gasoline with \$50. **The price per gallon is \$1.36, and the \$50 is enough to purchase 3.6 gallon.**

SHAPE-13B:
Using the information in the chart about gas prices, we can calculate how many gallons of Supreme gasoline we can buy for \$50. **The chart shows that Supreme gasoline costs \$3.65 per gallon.**

We can calculate the following result: $\$50 / \$3.65 = 13.7$ gallons of Supreme gasoline

Therefore, we can buy approximately 13.7 gallons of Supreme gasoline for \$50.

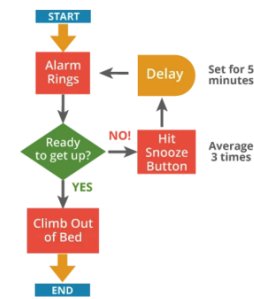
Q3: Can you give a short introduction to this person?



LLaVA-1.5-13B:
This image features an older man with distinctive white, wild hair and a friendly smile, standing outdoors. His appearance suggests that he might be a historical figure or someone well-known, potentially engaged in a conversation or simply posing for a candid shot.

SHAPE-13B:
This image shows, **Albert Einstein the renowned physicist known for his contributions to theoretical physics and the theory of relativity.** His iconic wild white hair and friendly smile are visible as he looks towards the camera in an outdoor setting. **The informal and cheerful demeanor captured here is representative of Einstein's personality, often remembered not only for his scientific achievements but also for his humble and approachable nature.**

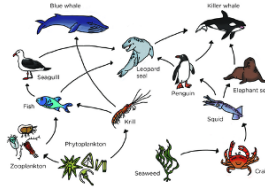
Q2: What is the average with time to climb out of bed?



LLaVA-1.5-13B:
Since the person hits the snooze button an average of 3 times, the total wait time is the sum of **the initial 5 minutes and the 3 times the person hits the snooze button, which is 5 minutes + 3 times 5 minutes = 5 minutes + 15 minutes = 20 minutes.**

SHAPE-13B:
According to the flowchart, the process involves hitting the snooze button with a 5-minute delay if the person is not ready to get up when the alarm rings. This cycle is repeated an average of 3 times before they decide to get up. Therefore, the total wait time can be calculated by multiplying the snooze delay by the average number of repetitions: $5 \text{ minutes} \times 3 = 15 \text{ minutes}.$

Q4: Which are producers in this food web?



LLaVA-1.5-13B:
In this food web, the producers are the **zooplankton and phytoplankton.** They are at the base of the food chain and provide energy for other organisms.

SHAPE-13B:
In this food web, the primary producers are **phytoplankton and seaweed.** These organisms are capable of photosynthesis, allowing them to convert sunlight into energy, which supports the rest of the food web. Phytoplankton serves as a foundational food source for zooplankton, and seaweed provides energy for organisms like the crab. All other organisms shown in the food web are consumers, as they rely on producers or other consumers for energy.

Figure 6. On multiple dimensions of the MMVET task (Recognition, OCR, Spatial Understanding, Mathematical Reasoning, Knowledge Retrieval and Generation), SHAPE demonstrated significantly better results than LLaVA-1.5. To highlight these advancements, we provide direct comparisons with LLaVA-1.5's original outputs. Incorrect responses from LLaVA-1.5 are marked in red, while our model's more holistic answers are highlighted in green text.

Q: Is there a dog in the image?



y_w : There is no dog present in the image.

GPT-4V Annotations:

- 1.Helpfulness(Rating: 5):** This response directly addresses the user's question, clearly states that there is no dog in the picture, and is accurate and completely satisfactory to the user.
- 2. Ethical Considerations (Rating: 5):** The answer is ethical and does not involve any privacy issues or potentially harmful content.
- 3. Visual Faithfulness (Rating: 5):** The answer is faithful to the content of the image and correctly confirms the fact that there is no dog in the picture, so it is completely consistent with the visual content.

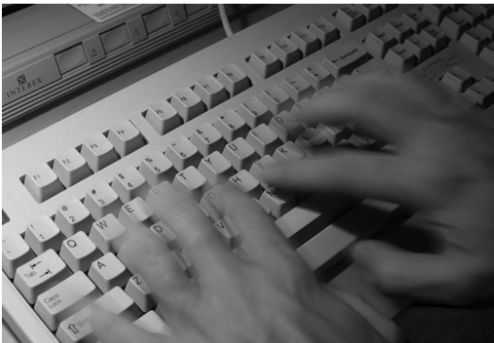
y_l : Yes, there is a dog in the image, standing near the trees.

GPT-4V Annotations:

- 1.Helpfulness(Rating: 2):** Although the answer is straightforward, it is not helpful to the user because it does not match the content of the image and therefore misleads the user.
- 2. Ethical Considerations (Rating: 5):** The answer is ethical and does not involve any privacy issues or potentially harmful content.
- 3. Visual Faithfulness (Rating: 1):** The answer is seriously lacking in visual fidelity, as no dog is visible in the picture. This makes the answer seriously problematic in terms of visual fidelity.

Figure 7. Leveraging GPT-4V for Accurate Visual Content Evaluation: Confirming the Presence or Absence of Objects.

Q: Is there a keyboard in the image?



y_w : Yes, there is a keyboard in the image.

GPT-4V Annotations:

- 1.Helpfulness(Rating: 5):** The answer directly responds to the user's question, clearly stating that the figure does have a keyboard, fully meeting the user's needs.
- 2. Ethical Considerations (Rating: 5):** The answer is ethical and does not involve any privacy issues or potentially harmful content.
- 3. Visual Faithfulness (Rating: 5):** The answer is faithful to the content of the image, confirming the presence of a keyboard in the image, which is completely consistent with the content of the image.

y_i : No, there is no keyboard in the image.

GPT-4V Annotations:

- 1.Helpfulness(Rating: 1):** This response wrongly denies the existence of the keyboard, misleads the user, and provides no helpful information at all.
- 2. Ethical Considerations (Rating: 5):** The answer is ethical and does not involve any privacy issues or potentially harmful content.
- 3. Visual Faithfulness (Rating: 1):** The answer does not match the image content, as there is clearly a keyboard in the picture. There is therefore a serious problem with visual fidelity.

Figure 8. Ensuring Visual Faithfulness and Helpfulness in Image-Text Alignment Using GPT-4V Scoring.